1-1-2015

Field Measurements for Remote Sensing of the Cryosphere

Hans-Peter Marshall
Boise State University

Robert L. Hawley
Dartmouth College

Marco Tedesco
City College of New York, City University of New York

14 Field measurements for remote sensing of the cryosphere

Hans-Peter Marshall[1], Robert L. Hawley[2] and Marco Tedesco[3]

[1] Boise State University, USA
[2] Dartmouth College, Hanover, USA
[3] The City College of New York, City University of New York, New York, USA

Summary

Remote sensing observations of the cryosphere, like any other target of interest, require ground-based measurements for both calibration and validation, as inversion algorithms are usually underdetermined and uncertainties in the retrieval are needed for application. Field-based observations are performed in selected representative locations, and typically involve both direct *in situ* measurements of the physical properties of interest, as well as ground-based remote sensing techniques.

New state-of-the-art modern techniques for measuring physical properties rapidly and at high spatial resolution have recently given us a new view of spatiotemporal variability. These are important, as large variability at scales below the typical footprint of spaceborne sensors often exists. Simulating remote sensing measurements using ground-based sensors provides the ability to perform both *in situ* and remote sensing measurements at the same scale, providing insight into the dominant physical processes that must be accounted for in inversion models and retrieval schemes.

While direct *in situ* measurements provide the most accurate information about the properties of interest, they are time-consuming and expensive and are, therefore, only practical at relatively few locations, and often with low temporal resolution. Spatial sampling strategies, designed specifically for the remote sensing observation of interest, can reduce uncertainties in comparisons between ground-based and airborne/spaceborne estimates. Intensive remote sensing calibration and validation campaigns, often associated with an upcoming or recent satellite launch, provide unique opportunities for detailed characterization at a wide range of scales, and these are typically large international collaborative efforts.

This chapter reviews standard *in situ* manual field measurements for snow and ice properties, as well as newer high-resolution techniques and instruments used to simulate airborne and spaceborne remote sensing observations. Sampling strategies and example applications from recent international calibration and validation experiments are given.

Field measurements are a crucial component of remote sensing of the cryosphere, as they provide both the necessary direct observations of the variables of interest, as well as measurements that simulate the particular remote sensing technique at scales that can be characterized accurately. Ground-based observations provide the information needed to:

1 improve and develop new retrieval algorithms;
2 calibrate algorithms; and
3 validate results to provide accurate uncertainty assessments.

14.1   Introduction

Remote sensing observations of the cryosphere, like any other target of interest, require ground-based measurements for calibration and validation (Figure 14.1). For example, many remote sensing inversion algorithms require estimates of surface and subsurface properties for calibration, and field-based observations are consequently performed in locations assumed to be as representative as possible of the target studied from space. Moreover, to evaluate the accuracy and limitations of remote sensing results, direct measurements of the physical properties of interest are required and performed in the field. Such field measurements are typically made manually by observers, or by automatic instrumentation.

This chapter begins with an overview of the physical properties of the cryosphere that are of interest and have a significant effect on remote sensing observations. We then cover techniques for measuring these properties, beginning with established standard techniques. We also describe new state-of-the-art modern techniques for measuring physical properties rapidly and at high spatial resolution, which have recently given us a new view of the variability of the sought parameters at different spatial scales, and often reveal large variability at scales below the typical footprint of spaceborne sensors.

A major complication with relating ground-based point measurements of physical properties to remote sensing observations is the mismatch in scale.

Figure 14.1 Example field campaign in support of remote sensing. Sea ice thickness measured with EM-31 in foreground, GPS base station on right, sled with GPS rover and ground based radar, snow pit observations on left, snow depth measurements in background (Photo by Matthew Sturn).

Indeed, an individual *in situ* measurement can be seen as representative of physical properties at a scale of the order of a few meters or even centimeters, while remote sensing observations are affected by areas and targets within the field of view of the instruments, ranging from several meters to tens, or even hundreds of kilometers. Simulating remote sensing measurements using ground-based sensors provides the ability to perform both measurements at the same scale, also providing insight into the dominant physical processes that must be accounted for in inversion models and retrieval schemes.

In order to relate ground-based measurements of physical properties to actual remote sensing observations at larger scales, sampling strategies must be developed to adequately cover the scale of the remote sensor footprint. These sampling strategies are discussed, and the chapter concludes with examples of field-based calibration and validation efforts made in recent years.

14.2   Physical properties of interest

It is obviously impossible to cover all the physical properties of interest for remote sensing of the cryosphere in a single chapter. In this section, we highlight some of the most important ones, hoping that this represents a valuable introduction for the reader interested in expanding his/her knowledge through the references reported below.

Remote sensing observations can be used to estimate a wide range of the physical properties of snow and ice, using both passive and active electromagnetic sensors and measurements of the Earth's gravitational field (http://climate2 .jpl.nasa.gov/ice/missions/; See also Chapters 10 and 15, for example). High-frequency electromagnetic waves can accurately probe the upper layers of firn (e.g., snow that has been left over from past seasons and has been recrystallized) and snow at high spatial resolution (Marshall and Koh, 2008), while lower frequencies can be used to probe the entire thickness of glaciers and ice sheets (Conway *et al.*, 2009). At a very large spatial scale, variations in the gravitational field can be used to estimate changes in the mass of snow and ice.

Any remote sensing estimate requires independent estimates of the physical property of interest for development and calibration. The most accurate estimates of these physical properties come from direct, ground-based *in situ* observations. These observations are usually destructive, time-consuming, and costly, and therefore can only be made at very limited temporal and spatial resolutions.

Geophysical instruments, which measure electromagnetic or acoustic waves, can be used to estimate properties from the ground at high spatial resolution and over much larger spatial scales than direct *in situ* measurements, and they improve the accuracy of estimates scaled from point observations to remote sensing footprints. These techniques are usually non-destructive. Sensors with the same characteristics as spaceborne instruments are also used on the ground and, due to their small footprint, the estimates deriving from such measurements can be more easily assessed and validated compared to *in situ* observations.

14.2.1 Surface properties

Accurate measurements of the elevation of snow and ice are used to monitor changes in mass of ice sheets (Abdalati and Krabill, 1999; Howat *et al.*, 2007), glaciers (Larsen *et al.*, 2007; Paul and Haeberli, 2008), and seasonal snowpacks (Deems *et al.*, 2006; Trujillo *et al.*, 2007). With estimates of elevation at many locations and at a range of scales, other topographic parameters can be calculated, including slope, aspect, and roughness. These are all important for estimating the energy balance for modeling, for example, melt and wind redistribution of snow. Slope estimates are required for ice flow modeling and calculating shear stress for avalanche studies, and surface roughness has a strong effect on passive and active microwave remote sensing, due to scattering of electromagnetic waves.

The ratio of outgoing to incoming solar radiation, termed *albedo*, is one of the most important parameters needed for energy balance modeling. Uncertainties in albedo often dominate model estimates of melt, so direct measurements are extremely valuable. Albedo measurements are usually produced as an integrated result over the shortwave portion of the electromagnetic spectrum. However, more accurate spectral measurements, which produce albedo estimates at many different wavelengths, are more useful, as they can provide validation and calibration data for the different channels at which spaceborne or airborne sensors collect information.

Surface temperature estimates can determine if snow or ice is melting and are the primary control on emitted radiation. The grain size of snow on the surface changes on a daily timescale and has a strong effect on albedo. The composition of the surface which, for the cryosphere, could be snow or ice, possibly mixed with water, dust or dirt, is also of interest. These observations can be used to indicate whether melt is occurring, and impurities are important as they can reduce the albedo drastically (e.g., darker material over the brighter snow and ice) and change the amount of solar radiation absorbed by the snowpack. Permafrost extent and depth would also be very valuable, but are still difficult to estimate with remote sensing (See Chapter 13).

Ice velocity is an important surface measurement for glaciers and ice sheets. These observations are used for ice flow modeling, for mass balance studies, and for monitoring the stability of ice (see Chapter 9). The height of sea ice above the water surface, called *sea ice freeboard*, is also an important surface observation, as it can be used to estimate sea ice thickness (see Chapter 11).

14.2.2 Sub-surface properties

Ground-based measurements of snow and ice properties below the surface are more difficult, as they require probing the sub-surface either destructively (e.g., digging snow pits) or using some type of short-range remote sensing. Destructive measurements are time-consuming and expensive, while remote observations require inversion algorithms that are often complex and can contain large uncertainties.

The most important subsurface property of a seasonal snowpack, from a hydrology perspective, is the snow water equivalent (SWE), or the amount of water resulting from melting all of the snow, which is defined as:

$$\text{SWE} = \int_{ground}^{surface} \frac{\rho(z)}{\rho_w} dz \tag{14.1}$$

where:

$\rho(z)$ is the snow density
ρ_w is the density of water
z is the direction normal to the surface
SWE is the water equivalent, in the same units as z.

The integration is performed from the ground (or previous summer surface) to the snow surface. The annual SWE is of interest for glaciologists and hydrologists, for example, as the SWE at the end of winter is input for the net mass balance at any point on a glacier or ice sheet, and represents the amount of water from snow available at the beginning of the melting season. Snow depth is a much easier measurement to make than SWE and has a larger variability than density over relevant spatial and temporal scales. Therefore, in general, often few density measurements are combined with a much higher number of depth observations, in order to produce many estimates of SWE.

The temperature profile within the snow and firn, another important sub-surface parameter, is the primary driver for snow metamorphism (McClung and Schaerer, 1993) in the near surface, where overburden pressures are low. Deep in the firn, in locations where temperatures remain below zero, the temperature profile can provide information about past climate. In areas where the melting point is reached, temperatures in the snow and firn can indicate melt regions, and these are necessary for estimating the energy input required to melt all of the mass. The deformation of ice also depends strongly on ice temperature, and ice temperatures can be used to infer past climate, due to the low thermal conductivity of snow and ice (Cuffey and Paterson, 2010).

The snowpack is made of many different layers, as each individual storm deposits a unique snow type. The saying "*No two snowflakes are alike*" comes from the fact that snow crystal formation is an incredibly complex process, with growth patterns that are extremely sensitive to temperature and humidity conditions. Snowflakes that reach the surface have passed through a wide range of conditions on their journey from the clouds. Once they reach the ground, they continue to change on a time scale of hours, depending on the environmental conditions. Changes occur faster at higher temperatures, and temperature gradients control the direction of snow grain growth.

While no two snowflakes from even an individual storm are alike, snowflakes from the same storm are much more similar to each other than to snow grains anywhere else in the snowpack. Before negligible melt occurs in the spring, the snowpack holds a stratigraphic record of the weather conditions during the previous fall and winter. In places where the snow never melts, such as the major

ice sheets in the Arctic and Antarctic, this record of local weather is preserved. Ice cores from the major ice sheets provide information about climate going back more than 400 000 years (Cuffey and Paterson, 2010).

Layering in snow and firn, termed stratigraphy, manifests through distinct changes in snow hardness, density, and microstructure. The major changes in these properties occur at boundaries between snowfall events, but they also vary within layers as well, although to a much lesser extent. These variations in snow morphology at the millimeter scale control the basic physical processes of snow heat flow, snow mechanics, and snow melt. Changes in grain size and shape, and the bonds between them, affect remote sensing observations, control avalanche formation, and cause complex water flow patterns within the snow. Due to capillary forces interacting with variations in snow microstructure, meltwater pathways form as isolated vertical columns, often with slope parallel flow at stratigraphic boundaries (Figure 14.2).

Liquid water content is a primary snow property of interest, and it can vary at the centimeter scale. Liquid water has an enormous effect on microwave remote sensing, as the electrical properties of snow change by more than an order of magnitude when snow becomes wet (see Chapter 2). Microwave sensors can detect the presence of melt easily, but estimating mass (SWE) in wet snow is not possible, due to the complexity of snowmelt processes (see Chapters 5 and 6).

Remote sensing observations of snow are also incredibly sensitive to variations in snow microstructure. Existing and proposed methods for measuring SWE from space are focused on measuring changes in passive or active radar measurements caused by electromagnetic signals being scattered by snow grains – termed *volume scattering*. As the mass of snow increases, more volume scattering occurs, which generally decreases passive microwave brightness temperatures and increases active microwave backscatter. There is a relationship between scattering and SWE but, clearly, there is also a very strong relationship between scattering

Figure 14.2 Frozen melt channels in polar firn. Capillary forces cause preferential flow paths within the percolation zone. Re-frozen melt channels shown as solid vertical columns; dry snow between has been removed. Meltwater is pooled at a stratigraphic boundary in foreground (Photo by Michael Demuth).

and snow microstructure. Information about snow grain size, type, and specific surface area, are therefore of interest throughout the snow and firn.

A glacier is divided up into different facies, depending on whether and for how long the location on the glacier has experienced melt. In the *dry snow facies*, the snow never melts; in the *percolation facies*, snow melts during the year but refreezes after melting; and in the *wet snow facies*, the snow experiences melt which moves mass beyond the current year in the stratigraphic record. At the lower end of the wet snow facies is the *slush facies*, where the snow is completely saturated with water, and the *superimposed ice facies*, where there is only ice in the summer. Active radar observations show a distinct change at the upper boundary of the percolation zone, due to the complex geometry of the liquid water pathways. Field observations at the end of summer are often used to determine glacier facies.

The thickness of ice, both on land and on sea, is of great interest to scientists studying the cryosphere. Estimates of ice thickness are needed for ice flow modeling, and sea ice thickness estimates are required for simulating annual sea ice distribution. Changes in the surface elevation of ice and snow on land can be measured with laser and radar altimeters. With an estimate of freeboard and accurate digital elevation models (DEMs), sea ice thickness can be estimated. More recently, intensive airborne remote sensing missions have measured land ice thickness using low frequency radar not available on current spaceborne platforms (http://www.nasa.gov/mission_pages/icebridge/index.html). Remote sensing missions which use repeat LiDAR can map snow depth by differencing surface elevations measured with and without snow cover (Deems *et al.*, 2006; Trujillo *et al.*, 2009). Other airborne missions use microwave radar to measure snow depth on sea ice (Farrell *et al.*, 2012).

First year sea ice is typically relatively smooth, while multi-year ice is often cracked and buckled, therefore the age of the sea ice is of interest. Crevasses and moulins on glaciers can control the glacier hydrology, give information about flow patterns, and cause scattering of electromagnetic signals (Conway *et al.*, 2002).

14.3 Standard techniques for direct measurements of physical properties

14.3.1 Topography

Surface topography is one of the most common remote-sensing measurements. Many traditional survey techniques have been employed to obtain surface topography in support of remote-sensing measurements. These include optical survey techniques, aneroid barometry, TRANSIT satellite (also known as NAVSAT, Navy Navigation Satellite System) and, more recently, the use of the Global Positioning System (GPS), one of several Global Navigation Satellite Systems (GNSSs).

When relative topography is desired, or the surface to be measured is geographically close to a known benchmark elevation, optical survey techniques can be used.

Figure 14.3 Sight leveling on Peyto Glacier, Alberta, Canada. The sight level is mounted on the tripod. The operator views a stadia rod through the telescope on the level, reading the markings on the rod to determine the distance from the reference plane to the surface. A handheld tape measure determines the distance between stadia rod placements. Another stadia rod is visible in the background, used by another survey team (Photo courtesy Dartmouth College Off-Campus programs).

Standard optical techniques include sight leveling and theodolite and Electronic Distance Measurement (EDM) surveying. In sight leveling, a surveyor's level is typically used. This device is essentially a telescope with crosshairs that rotates on a fixed plane (Figure 14.3).

The plane of the level is oriented normal to the geoid surface by using one or more bubble levels attached to the instrument. Once leveled, the telescope can rotate, and anything in the telescope crosshairs is at the same level. When combined with the use of a stadia rod or level staff (a staff marked with measurements along its length) and a standard surveyor's tape measure, profiles of elevation can be measured. To measure a profile, the level is placed near a high point in the profile and leveled. The stadia rod is placed on the first point to be surveyed. A reading of the elevation markings on the stadia rod through the telescope provides the elevation of the plane above the snow/ice surface. The rod is then moved to the next point. A second reading through the telescope provides the elevation of the reference plane above the surface at this point – the difference between the two is the difference in elevation between the two points. The distance between the points is measured with a standard surveyor's tape measure. After a series of measurements, the level can be moved to a new location, keeping the stadia rod fixed for one measurement, and a new reference plane is established. In this way, a long profile of surface topography can be constructed.

Sight leveling generally produces surface topography measurements that are inherently two-dimensional; elevation measurements are taken along a straight line. If elevation measurements of arbitrary points (not falling along a straight line) are desired, or if exact geographical co-ordinates are required for each elevation point, a more complete positioning system is needed. In optical surveying, a *theodolite* is used to make precise measurements of the angles (both vertical and horizontal) between target points of interest. In common use, the distance between the theodolite and each target is determined with *Electronic Distance*

Measurement (EDM), using a corner-cube reflector and electromagnetic radiation at several frequencies. When combined with angle measurement, this combination is often referred to as a *Total Station* (e.g., Kavenagh and Bird, 1996). When the angles, both vertical and horizontal, and the distances to each target point are both measured, a vector can be constructed to each surveyed point and, thus, each point can be located in 3D space relative to the others.

Optical techniques provide relative measures of topography, and a reference point is needed to determine absolute elevations. If a suitable rock benchmark is near enough to the survey area, an optical survey can be connected to the benchmark for absolute positioning. In some surveys, the closest benchmark is too far away to be practical, as with central locations on ice sheets. In such situations, an independent measure of surface elevation is required. Before satellite navigation became popular, elevations in remote locations were frequently measured using atmospheric pressure. Aside from the complications ensuing due to local pressure variations and weather patterns, an *aneroid barometer* can serve as a useful indicator of elevation. These instruments are sometimes termed *pressure altimeters*.

While early attempts at surveying via satellite positioning were cumbersome (e.g., TRANSIT/NAVSAT), the more modern GPS (as mentioned, one of the GNSS system) is now commonly used to make both absolute and relative measurements of topography. A GNSS receiver determines its position in space by measuring the distance between itself and the satellites in the GNSS "constellation". The distance measurement is made by analyzing "pseudo-random" code transmitted by the satellite to determine the time-of-flight between the satellite and receiver (http://en.wikipedia.org/wiki/Global_Positioning_System). With distances to at least four satellites, a position fix can be made. While this is a minimum for an accurate fix, in typical usage, a receiver tracks many more satellites of the 24-satellite GPS constellation at any given time.

Normal GNSS receivers can produce a fix in real time, but the position information is generally only accurate to within several meters or even tens of meters, even with the best receivers. There are several reasons for this level of accuracy. The positions of the satellites themselves, or *ephemeris*, are measured precisely by ground stations, but these precise measurements are not available in real time. Instead, navigation receivers rely on *broadcast ephemeris* transmitted by the satellite itself to determine positions. In addition to errors in the ephemeris data, the atomic clocks on each satellite experience slight drift which, while it can be measured, cannot be determined in real time. In addition to these measurable errors, an additional error is introduced by the propagation of the GPS signal through the Earth's ionosphere. This causes path delays to the signal, and these delays are affected by the changing patterns in the ionosphere.

To achieve survey-grade (cm-level) accuracy, rivaling the measurements made by optical techniques, a *survey grade* GNSS receiver is used. These receivers continuously record the GPS/GNSS signals from the satellites in view, to be downloaded for further post-processing. In post-processing, software can use *precise ephemeris*, measured as the satellite passes over ground stations of known

Figure 14.4 GPS survey setup used by Seigfried *et al.* (2011). The survey-grade GPS antenna is mounted high on the sled towed behind the snowmobile, which provides a clear sky view and prevents the bouncing that would be associated with a mounting point on the back of the snowmobile itself. Additionally, the length of the sled integrates surface roughness at the scale of the sled (Photo by Bob Hawley).

location, rather than the less accurate broadcast ephemeris. This enhances the accuracy considerably. In addition, since the receiver continuously records satellite data, it is possible to occupy a position for a very long time, (12–24 hours), long enough for ionospheric disturbances to change, and thus for the delays associated with them to change. This long occupation is known as a *static* measurement, and can result in centimeter accuracy.

In situations where multiple points are to be surveyed, it is common to survey a single point using the static method, and then measure the *baselines* between that point and every other point, using *differential* processing. In differential processing, two or more receivers are used to simultaneously record satellite data at different points. Because, at the scale of the survey, the signals traveling from the satellite to each receiver are passing through the same ionosphere, errors in the *difference* between the two positions due to the ionosphere can be eliminated. Additionally, because the length and angle of the baseline is required in a differential measurement, rather than absolute position, errors from satellite ephemeris are also eliminated. One result of this is that accurate baselines (1–3 cm) can be measured with a much shorter occupation time, often 10–20 minutes. This measurement style is known as *fast static*. In recent years, high spatial resolution surveys of topography have become possible using *kinematic* data collection and processing (King, 2004), described in section 14.4.1. Figure 14.4 shows a survey-grade GPS unit mounted to the top of a sled for fast static and kinematic measurements.

14.3.2 Snow depth

Snow depth is monitored, in the simple case, at a fixed point by frequently making a reference measurement throughout the year. In a seasonal snowpack, this can be typically done with an ultrasonic sensor which monitors the location of the snow

surface (DeWalle and Rango, 2011). On a glacier, measurements of the height of an ablation stake are made (Cuffey and Paterson, 2010). Destructive measurements are made spatially with a probe at lower temporal resolution, and are possible up to a depth of approximately 10 meters. These measurements can be made in the ablation zone on a glacier, but it can be very difficult in the accumulation zone to distinguish the previous year's surface by detecting a change in hardness. In this situation, snow pits or shallow cores (up to 15 meters) are required to estimate snow depth.

14.3.3 Snow water equivalent and density

As mentioned, snow density is required, in addition to depth, for estimating the mass or SWE. This involves taking snow samples of known volume and weighing them, by carefully filling density cutters with appropriate procedures, for a direct destructive measurement of density. Since density is much more time-consuming to measure, and is assumed to vary spatially and temporally less than depth, an order of magnitude more depth measurements than density measurements are usually available. Density cutters vary in size from $10\,\mathrm{cm}^3$ to $1000\,\mathrm{cm}^3$. Small sizes are used to measure density in small thin layers, usually for avalanche applications, while large cutter sizes do a better job of accurately sampling the average density of the snowpack. These cutters are used to take samples at equal depth intervals in a snow pit, with depth varying from approximately 30 cm to 3 meters.

Snow density can be also measured with a coring device. In seasonal snow, the core is pushed into the dirt at the base of the snowpack, which acts as a plug to prevent snow from falling out of the tube, and the dirt plug is removed before weighing. The core is weighted, with and without the snow, and the SWE can be estimated from the differences in the weights. This works well in cold conditions where soil exists, but is much more challenging in warm weather and at snow-rock interfaces. At several hundred locations around the western USA, SWE is measured continuously by weighing a location of several square meters with a glycol-filled "pillow" and a pressure sensor (http://www.wcc.nrcs.usda.gov/snow/).

In the polar regions, shallow cores, typically 10–30 meters long, are extracted using a larger diameter core barrel (see Figure 14.5). These samples are cut into sections and weighed for density. Density observations are also made on deeper ice cores, providing density measurements throughout the firn.
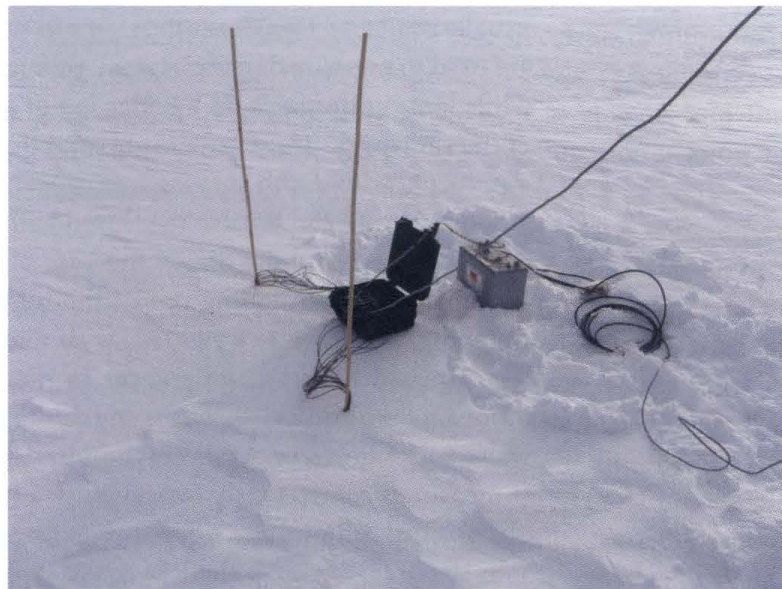
14.3.4 Temperature

Temperature observations in snow are straightforward. Typically, a dial stem thermometer is inserted into the sidewall of a snow pit, and a temperature measurement is made every 5 cm. Near ice layers and weak layers, temperature might be measured in more detail to estimate the temperature gradient influencing metamorphism. Strings of thermistors are often deployed at weather stations

Figure 14.5 Removing the core from the core barrel at a shallow firn coring operation at Kongsvagen, Svalbard. The drilling head is to the right, and the core is extracted through the opposite end of the barrel into the waiting tray. The core protruding from the drilling head is a result of slippage of the "core dogs" when extracting the core after a drill run. The density data from this core is shown in Figure 14.12 (Photo by Bob Hawley).

Figure 14.6 Thermocouples for measuring surface and subsurface temperature. Brown wires are individual thermocouples leading to the black box containing the datalogger and multiplexer. The setup is powered by the single deep-cycle battery to the right of the box, which is charged by a solar panel (not pictured) (Photo by Bob Hawley).

to make subsurface temperature measurements in snow and firn continuously. Temperature measurements within boreholes are made to monitor temperatures in the snow, firn, and ice to much greater depths (Figure 14.6).

14.3.5 Stratigraphy

Stratigraphy is much harder to observe and the observations are more subjective. Typically, individual storm layers are identified using a hand-hardness test, on a scale from 1–5, using a fist, fingers, and a pencil with a small amount

of pressure. Within each layer, snow grain size and shape are estimated using a hand lens. Stratigraphy in snow pits is measured from the surface to the ground in seasonal snowpacks, and within the upper two meters typically in polar regions (Figure 14.7a). The International Classification for Seasonal Snow on the Ground (Fierz *et al.*, 2009) and other observational guidelines (Greene *et al.*, 2010) are valuable references for anyone performing ground-based snow observations. Sometimes, samples are cast by filling the void space with a chemical liquid that freezes immediately and preserves microstructure (Figure 14.7b). These samples are analyzed in detail in a lab using thin sectioning, surface sectioning techniques and, more recently, X-ray tomography. This process is very time-consuming and less common, but it provides detailed information on the snow microstructure.

14.3.6   Sea ice depth and ice thickness

Sea ice depth is commonly measured by coring the ice for a manual measurement. Drilling to the bed on glaciers and ice sheets also provides a destructive method for measuring ice thickness. Both are very time-consuming, so this is performed at relatively few locations. Low frequency radars are so commonly used for measuring land ice thickness that they are a standard technique. We will discuss this measurement strategy in the next section with the other radar techniques.

14.4   New techniques for high spatial resolution measurements

14.4.1   Topography

Advances in technology have made very high spatial resolution measurements of topography possible. Although some of these techniques technically qualify as remote sensing in themselves, we deal with them here because they are often used in remote-sensing ground-truthing campaigns. One such technique is terrestrial Light Detection And Ranging (LiDAR). Many terrestrial LiDAR systems are available; most mount on a standard survey tripod and can be automated to scan areas from tens of meters to several kilometers. As the scanning head of the LiDAR unit moves, it collects range, azimuth, and elevation information from a given reflector, thus recording a three-dimensional vector from the scan head to the ground point.

The difference between terrestrial LiDAR and theodolite measurements is that, instead of surveying specialized survey targets which have to be manually moved, the LiDAR receives reflections from almost all surfaces and objects around, allowing measurements of more than 100 000 points to be collected in a matter of hours. A set of these vectors defines the relationship of each ground point to the others, and a digital elevation model (DEM) can be constructed from these points.

Figure 14.7 Left panel (A): typical snow pit size. Note ruler and thermometers on pit wall to the left (Photo by Bob Hawley). Right panel (B): Casting a snow sample. The sample is placed in a liquid-tight container. Dimethyl phthalate is added slowly to a corner of the extracted sample to allow the chemical to fill from the bottom, preserving the microstructure for later laboratory analysis (Photo by HP Marshall).

This DEM has several uses in the context of larger remote sensing campaigns, and it has a much higher spatial resolution than remotely sensed elevation data from airborne and spaceborne platforms. Surface roughness is a critical parameter in many remote-sensing applications, and a terrestrial LiDAR-based DEM can be queried to determine roughness on any number of scales, in any number of directions.

Advances in processing strategies have also allowed GPS/GNSS surveys to become not only higher-resolution, but also simpler to run in the field. *Kinematic* processing of GPS data allows a pair of receivers to measure positions at very high

frequency, eliminating the stops required by the fast static method described in the previous section. As with other differential GPS measurements, kinematic GPS determines a tridimensional vector between two receivers. One receiver is fixed for the duration of the survey, and is known as the *base* station. The other receiver moves over the terrain of interest, and is known as the *rover* station. Kinematic processing can be performed in post-processing (*post-processed kinematic or PPK*) or, using receivers equipped with a radio link, in real time (*real-time kinematic or RTK*).

For PPK surveys, the field procedure is very simple; start the two receivers, allow some time to elapse while both are collecting data (initialization time), and then move the rover over the terrain of interest. PPK data can then be processed into an X, Y, and Z position for each GPS measurement collected. Common survey strategies using this technique are to establish a base station receiver, allow it to collect enough data (6–24 hours) for *static* processing (see previous section), allowing the survey to be connected to a global reference frame, and then walk, ski, or drive the roving receiver in a grid pattern over the surface of interest. The exact nature of the grid is dependent on both the surface topography to be measured and the remote-sensing platform (see section on sampling strategies below).

14.4.2 Surface properties

Surface properties to be measured in the field can be divided into two categories:

- First, simultaneous measurement of electromagnetic properties (simulating an airborne or spaceborne instrument) and the physical properties inferred from the electromagnetic properties (e.g., measuring spectral albedo and grain size simultaneously).
- Second, manual measurements of properties that *affect* remote sensing measurements, but for which no simultaneous measurement is possible (for example, measuring surface roughness to see how it affects a radar altimeter).

There are many instruments for collecting measurements of the surface electromagnetic emission or reflectance. The *radiometer* is the most general of these. Radiometers carried aboard aircraft and satellites are the basis for many remote sensing techniques. Smaller versions of the same instrument have taken many forms. Broadband radiometers are commonly found on Automated Weather Stations (AWSs), where they measure both the *downwelling* (incoming) radiative flux (when pointing up) and the *upwelling* (reflected or emitted) flux (when pointing down). The ratio of these measurements is a measure of *albedo*, an important property in itself and for remote sensing studies.

Narrow-band radiometers for specific ground-truthing measurements in satellite frequency bands, such as the LandSat bands (see Figure 7.1), are also available. These allow measurements of specific surfaces at these frequencies, to assist in classification in the remotely-sensed image. Since many remote-sensing classifications employ band ratios to avoid the problems caused by path

radiance, *ratioing radiometers* allow these ratios to be measured more directly (http://archive.org/details/nasa_techdoc_19840071065). In such a measurement, the user selects the bands to be ratioed and aims the instrument at a target, and the ratio is displayed.

To measure a wide spectrum of electromagnetic reflectance of a target, handheld *spectrometers* are used. Similar in measurement technique to the ratioing radiometer, the spectrometer is aimed at a target and a spectrum is acquired – a measurement of the intensity of electromagnetic radiation emanating from the target, in a large number of narrow bands. This allows a much more detailed classification of the material to be analyzed. Since the spectrum of a target is inherently dependent on the spectrum of the electromagnetic source, it is advisable to collect also the spectrum of the direct incoming electromagnetic radiation – essentially collecting a measurement "looking up". Differencing or ratioing these two measurements results in an actual *reflectance spectrum*, a property of the material itself, and predominantly independent of the electromagnetic source. Since this type of measurement is common and important, this differencing is frequently done in the acquisition software. Calibration measurements are also made in the field using targets with known albedo.

Measuring physical properties of the surface can be critical to any ground-truthing effort. Many physical property measurements undertaken in snow pits (see section 14.3.2) can be duplicated at the snow surface. An important measure for many ground-truthing studies is small-scale topography, or surface roughness. As discussed in the previous section, high-resolution local topography can be measured with a ground-based LiDAR instrument. Simpler techniques are also available. Albert and Hawley (2002) used a simple blade, 3 m in length, inserted into the snow. The top surface of the blade was made level, and a profile of the distance from the top of the blade to the snow surface, along the length of the blade, provides a measurement of the snow surface topography at the local scale. Lacroix *et al.* (2008) used a laser ranging device mounted on tracks to measure a similar profile of surface roughness.

Surface roughness can be determined digitally from standard visible-light photography of the snow surface using a board placed in the snow vertically (Fassnacht *et al.*, 2009). Time-lapse studies of changing snow surfaces can provide a time series of the evolution of surface roughness. New technologies, such as the Xbox360® Kinect® sensor (Mankoff *et al.*, 2011), may soon be adopted to obtain quantitative time-lapse information of the changing surface.

14.4.3   Sub-surface properties

High-resolution ground-based techniques for subsurface measurements either 1) require access to the subsurface via a snow pit or borehole, or 2) utilize a ground-based remote sensing method. The first requirement means that these techniques are effectively *in situ*, and the measurement is made very close to the snow it samples. The second requirement means that inversion algorithms and

interpretation are necessary before subsurface properties are estimated. They allow rapid, non-destructive measurements, but require extensive data analysis and post-processing. The major advantage over airborne and spaceborne remote sensing is that the footprint is small and, therefore, ground calibration and validation is much more accurate and easier to interpret.

### 14.4.3.1   In situ measurements of sub-surface properties

At the smallest spatial scale and highest spatial resolution is the relatively new technique of X-ray tomography on snow samples (Kaempfer *et al.*, 2005; Lomonaco *et al.*, 2011; Schneebeli and Sokratov, 2004). This, indeed, provides a spatial resolution of micrometers, on samples up to the 10 cm scale. This high-resolution technique improves upon previous methods for studying snow at this scale, which includes surface and thin sectioning of cast snow samples (see Figure 14.7(B)). X-ray tomography can be performed on undisturbed samples, and environmental conditions can be controlled during time-lapse experiments. These studies are giving snow scientists a new view of microstructure and metamorphism.

At the snow pit scale, observations have advanced significantly with respect to spatial resolution, with the aid of near-infrared (NIR) photography for recording stratigraphy through differences in grain size-dependent reflectivity in the NIR band (Matzl and Schneebeli, 2006). Figure 14.8 shows a set-up for NIR photography on the Greenland ice sheet. Careful calibration can lead to estimates of Specific Surface Area (SSA), or the surface area to mass ratio, which controls both albedo and chemical reactions between the snow and the atmosphere. However. estimates are also sensitive to grain shape, which also needs to be taken into account (Gallet *et al.*, 2011). Broadband contact spectrometry has also been used by researchers to measure the spectral albedo of snow on a snow pit wall (Painter *et al.*, 2007). As in the description of spectrometry for surface characterization, this technique involves measuring the wall of a snow pit with a known light source, and can provide a vertical profile of SSA.

Borehole measurements allow some of the observations normally carried out in snow pits to be performed at greater depths. Measuring stratigraphy can be accomplished using a simple borehole video camera. Borehole Optical Stratigraphy (BOS) is a combination of a downward-looking video camera and post-processing software that allows interpretation of visual stratigraphy in a borehole. Hawley *et al.* (2003, 2008) used BOS to determine annual layering in Antarctica and Greenland, though its initial design goal was to track optical features through time. Because a borehole can remain accessible for long time periods, it is possible to make repeated measurements. As the firn column compacts, optical features move closer together. Hawley and Waddington (2011) demonstrated that optical features could be tracked through time to determine a profile of vertical strain and thus firn compaction. Figure 14.9 shows BOS in action on the Greenland ice sheet.

Neutron scattering in boreholes has been shown to provide accurate estimates of snow density (Morris and Cooper, 2003). A radioactive source and detector

Figure 14.8 Near-infrared photography set-up on the Greenland Ice Sheet. Note the layering visible at the bottom of the pit wall, the mount in the foreground to keep the camera still, the ruler for georeferencing, and the calibration targets and flat field surface on the pit wall. The pit is covered with fabric that lets diffused light only into the pit (Photo by Eric Lutz).
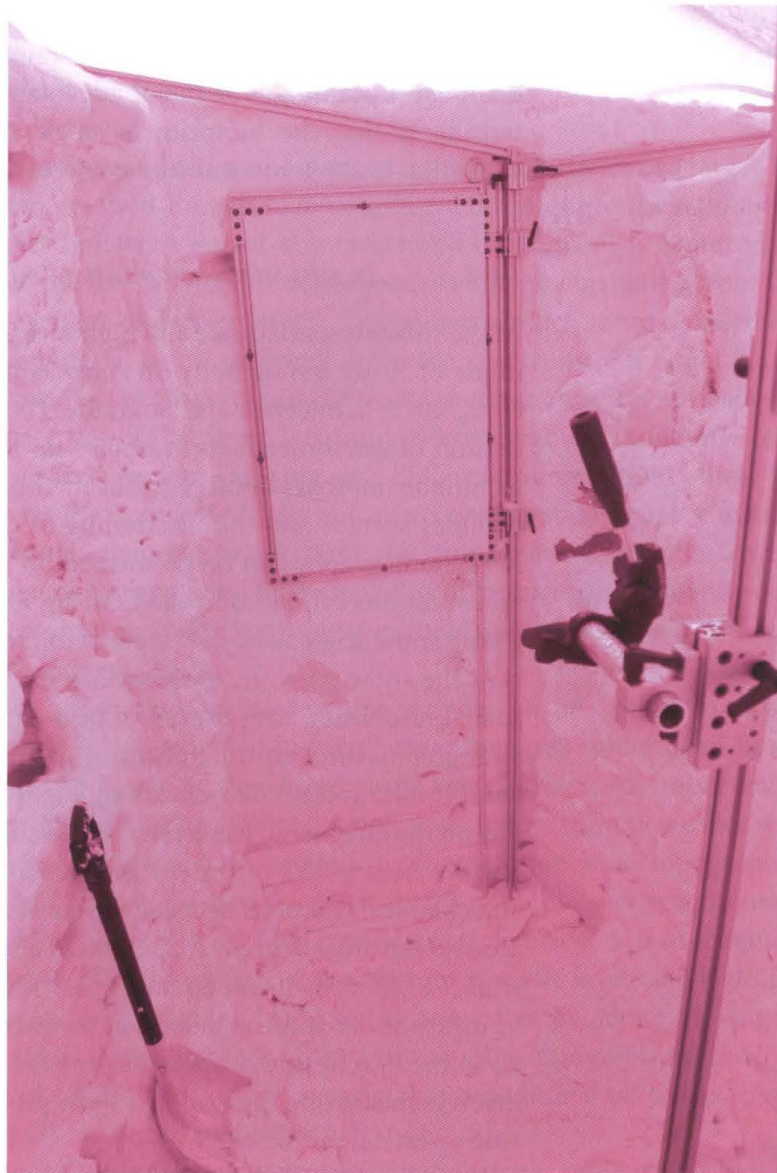
are lowered into the borehole, and neutrons scattered back to the detector are measured. The instrument, called a Wallingford Probe, was originally designed to measure soil moisture. Fast neutrons are scattered by hydrogen atoms, and the number of neutrons measured at the detector is related to the density of the medium. A similar technique is used in seasonal snowpacks, in which scattered gamma radiation is used to measure SWE either at a fixed location or from an aircraft. The difference with the gamma sensor is that an integrated value is estimated and, therefore, the scan can be performed remotely (see section on SWE or snow depth retrieval from more details).

Firn cores are typically scanned with optical sensors after they are extracted to locate annual layering, as the fall surface typically can be distinguished from

Figure 14.10 Figure 2 from Hawley *et al.* (2008); measurement of density on multiple length scales. Panel A: density measurements made on individual core sections in the field. Panel B: Grey line, same as panel A. Black line: density as measured in the borehole by a Wallingford neutron-scattering probe (Morris and Cooper, 2003). Note the slight smoothing of the stratigraphic signal. Panel C: Grey line, same as panel A. Black line: density as calculated from the dielectric profile (DEP) measured in the lab. Note how DEP resolves fine-scale ice layers that are only subtly seen in panel B. Panel D: optical imagery of core sections, for stratigraphic reference. Clear ice sections appear dark, and snow and firn appear light. (Hawley *et al.*, 2008. Reproduced with permission of International Glaciological Society).
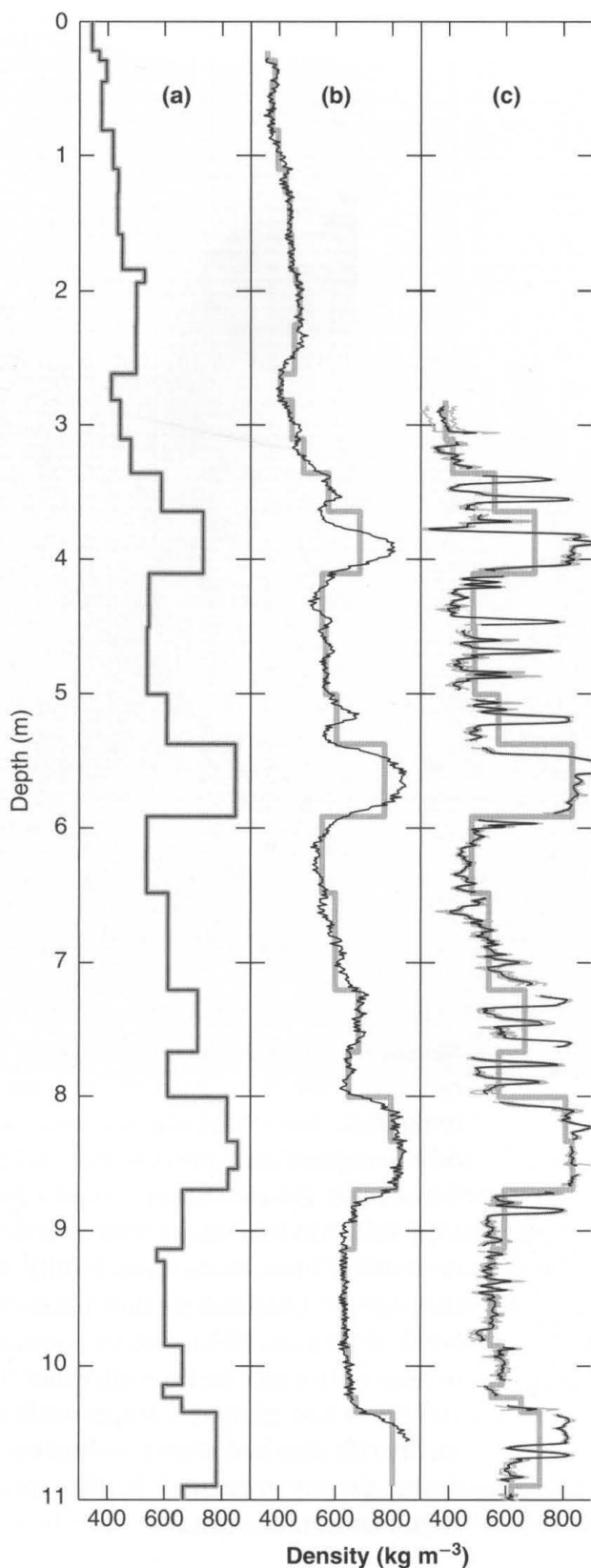
Figure 14.9 Borehole logging with a Borehole Optical Stratigraphy tool. The cable runs from the spool over the pulley mounted on the survey tripod, and down the hole to the instrument. The depth of the instrument is measured by an optical encoder mounted on the pulley (Photo by Gifford Wong).

the snow deposited during the winter. Dielectric measurements of conductivity on cores have been used to estimate density and changes in chemistry and impurities. More sophisticated techniques for measuring properties on a firn core have been developed, which include the Maine Automated Density Gauge Experiment (MADGE) and Mostly Automated Borehole Logging Experiment (MABLE). MADGE uses scattered gamma radiation, similar to the technique used in seasonal snow, to measure density at high resolution (3.3 mm) and precision (0.003 g/cm^3). MABLE is a down-hole technique that measures the hardness of the borehole wall and NIR reflectance, and it is used as a tool to determine the location of missing firn core sections after they have been extracted (Breton *et al.*, 2009).

Figure 14.10 illustrates length-scale issues, comparing density measurements made with standard coring techniques to density measured with a Wallingford Probe, density measured on the core using Dielectric Profiling, and optical stratigraphy on the core.

In seasonal snow, a penetrometer technique has been developed, which measures snow hardness at 0.004 mm resolution (Johnson and Schneebeli, 1999; Schneebeli *et al.*, 1998). Statistical methods have been developed that use the hardness profile to estimate density and texture index (Pielmeier *et al.*, 2001), and the hardness profile has been used for ground truth of ground-based radar stratigraphy (Marshall *et al.*, 2007). The recorded hardness profile also contains detailed information about grain bond strength, and the signal can be inverted for microstructural and micromechanical properties (Johnson and Schneebeli, 1999; Loewe and Herwijnen, 2012; Marshall and Johnson, 2009).

Figure 14.11 shows an example of snow micro-penetrometer (SMP) profile, with the hardness of the entire profile and a zoomed-in region showing the sub-millimeter detail in this data. These microstructural and micromechanical properties have been used to classify the stability of a slope (Lutz *et al.*, 2009; Pielmeier and Marshall, 2009), and to statistically classify grain type (Havens *et al.*, 2013; Satyawali & Schneebeli, 2010; Satyawali *et al.*, 2009). While developed for a snow avalanche application, this instrument is valuable for remote sensing calibration and validation field campaigns, as it provides accurate, quantitative measurements that are sensitive to snow microstructure.
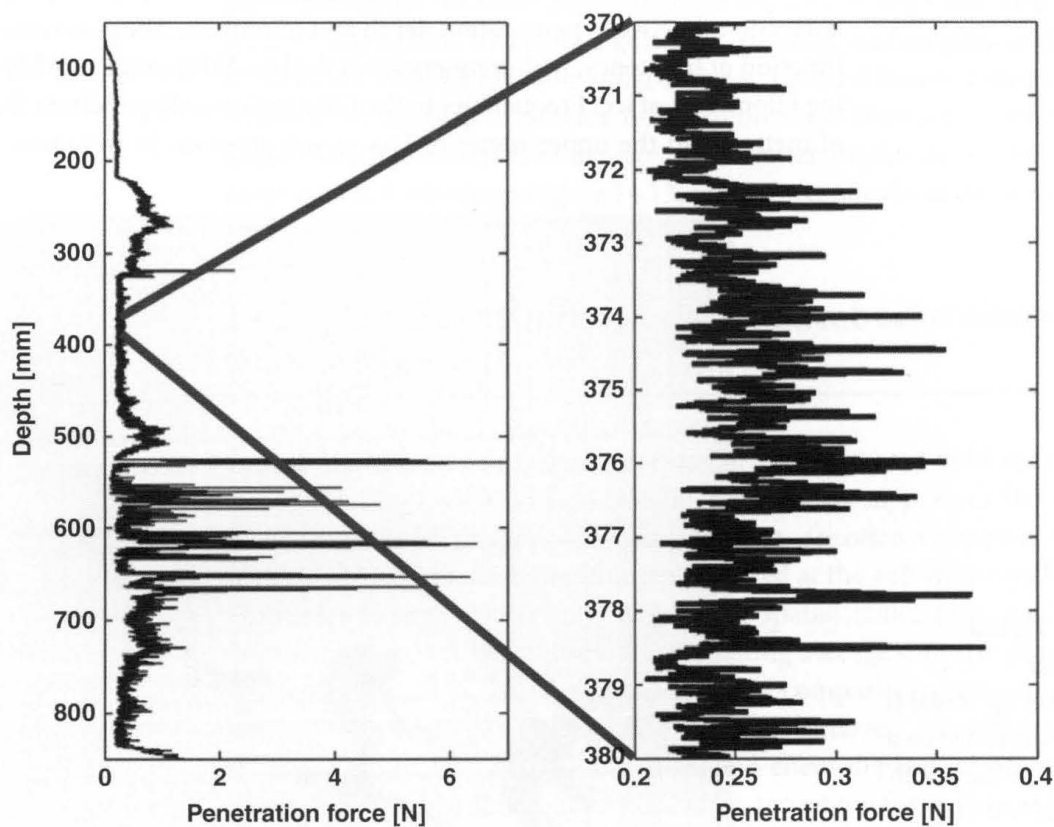

Figure 14.11 Example SMP profile in 85 cm snowpack showing layer hardness on the left, and 1 cm of data shown in detail on the right. Note the large ice crusts between 500 and 700 mm, and the individual ruptures in the zoomed-in area.

14.4.3.2 Ground-based remote sensing of sub-surface properties

The observation that snow and ice was fairly transparent to radio waves dates back to 1933. In 1957, after complaints from pilots about radar altimeters not working over snow and ice, the US Army conducted a study which showed that ice thickness of polar glaciers could be measured with a 440 MHz radar altimeter. In the 1960s and 70s, many ice-penetrating radars were built, and the technique is now standard for mapping ice thickness, both on Alpine glaciers and on polar ice sheets (Evans and Robin, 1972; Robin *et al.*, 1969; Waite and Schmidt, 1962).

Recent ground-based and airborne radar campaigns have mapped ice thickness and internal stratigraphy of glaciers and ice sheets (Gogineni *et al.*, 2007; Holt *et al.*, 2006; Vaughan *et al.*, 2008; http://www.nasa.gov/mission_pages/icebridge/index .html), and radar data have been used to infer past patterns of accumulation and histories of ice-sheet dynamics (Conway *et al.*, 2002; Nereson and Raymond, 2001; Waddington *et al.*, 2007). More recently, microwave radar has been used to measure snow stratigraphy and snow water equivalent in both seasonal and polar snowpacks (Marshall and Koh, 2008). Figure 14.12 shows a microwave radar measurement set-up, which is lightweight and allows two skiers to perform measurements with the radar over undisturbed snow.

When using ground-based radars for measuring snow and ice properties, there is a trade-off between penetration depth and resolution. The penetration depth is a function of frequency, with frequencies in the low MHz range capable of penetrating kilometers of ice. Frequencies in the GHz region only penetrate the upper tens of meters, and the upper meter or less in wet snow as, in wet snow, attenuation

Figure 14.12 Typical microwave radar measurement set-up. Radar is the white box suspended on a pole between two skiers, with control unit and batteries in a backpack. This allows measurements to be made easily in rugged alpine terrain (Photo by James McCreight).

is a strong function of frequency. Resolution is a function of bandwidth, or the range of frequencies over which a radar emits power. Bandwidths greater than an octave are difficult to achieve in practice, so therefore the bandwidth of most radar systems for cryosphere studies is at most of the same order of magnitude as the center frequency. Therefore, high-frequency systems can achieve much higher bandwidths, and provide therefore data at a typically higher vertical resolution. The center frequency also determines the sensitivity of the system to internal layering, heterogeneities in the subsurface, and liquid water, and ground-based radars operating at high frequencies typically have more narrow beams and, therefore, higher horizontal resolution.

In ground-based radar applications in the Cryosphere, 1–10 MHz radar systems are used to image the thickness of ice sheets and glaciers, 50–500 MHz systems are used in the firn and small glaciers, and microwave (1–18 GHz) radars are optimal for the upper 20 meters. Microwave systems also cover the range of current and planned spaceborne radar missions for snow (X- and Ku-bands, 8–18 GHz), so these measurements can provide data for direct comparison with airborne and spaceborne scatterometers.

Note that, from space, due to engineering limitations and Federal Communications Commission (FCC) regulations, active radar systems are limited to fairly low bandwidths. Internal reflections are difficult to separate from surface and ground returns, and inversion algorithms use integrated amplitude measurements at different frequencies and polarizations. Ground-based systems with larger bandwidths can help to provide information about the location and cause of the major contributions to the integrated backscatter amplitude. A typical microwave radar profile is shown in Figure 14.13, with power shown in dB.

14.5   Simulating airborne and spaceborne observations from the ground

One of the primary difficulties in relating ground-based field measurements to remote sensing observations is the difference in the *support*, or the footprint size of the measurements. Remote sensing products are often averages at the kilometer scale, while field measurements are performed at the sub-meter scale. Since snow properties change significantly over small spatial scales (e.g., 1–100 m), many field measurements are required for estimating average snow properties at remote sensing footprint scales, hence making the comparison between ground- and satellite-based estimates more complicated. Moreover, atmospheric parameters affect spaceborne measurements (with the effect depending on frequency and atmospheric parameters), which should be accounted for in the comparison.

In order better to understand the way electromagnetic signals interact with snow, ground-based instruments have been developed to simulate airborne and spaceborne observations, with the advantage of a very small footprint (e.g., Cline, 2000; Hardy *et al.*, 2008). The sensor must be located high enough above the snow surface
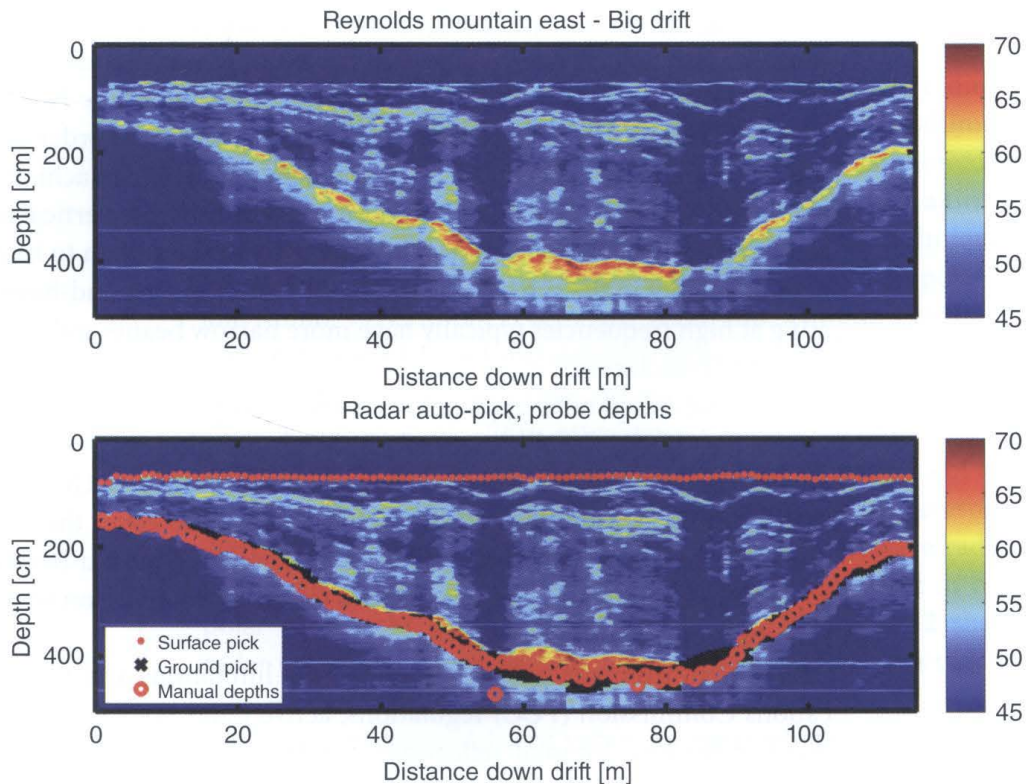
Figure 14.13 Typical microwave (2 – 10 GHz) radar profile. Top figure shows radar data, bottom figure shows locations of automatically picked surface and ground returns, and 118 manual measurements of snow depth. Note the internal stratigraphy that is resolved, and regions of low reflectivity likely caused by liquid water concentrations.

to be in the far-field, which is approximately $\frac{D^2}{\lambda}$, where D is the largest dimension of the antenna aperture and λ is the wavelength. Over this small footprint, detailed snow characterization can be performed and both forward electromagnetic models and inversion algorithms can be tested. Figure 14.14 shows a microwave radar suspended two meters above the snow surface in the far field for simulating airborne and spaceborne radar observations.

14.5.1 Active microwave

Experiments with tower mounted active radar scatterometers were performed in Europe and the US, and form the bulk of the existing data of radar backscatter in snow (Matzler *et al.*, 1997; Strozzi and Matzler, 1998; Ulaby *et al.*, 1977). Since those measurements, there have been few efforts to measure radar backscatter in a wide range of snow conditions, and the lack of data of this kind has severely limited progress with radar retrieval algorithms. Expanding the available data of radar backscatter in snow has been the focus of more recent snow remote sensing campaigns.

During the NASA Cold Land Processes Experiment (CLPX), in 2002 and 2003, several different tower-mounted radar systems were maintained at the Local Scale

Figure 14.14 Microwave radar measuring at 35 degrees incidence in far field. Radar is the white box on the far side of the sled. Control unit and batteries are located in boxes on the sled. Survey-grade GPS is mounted to the near side of the sled to avoid interference from radar (Photo by Hans-Peter Marshall).

Observation Site (LSOS) intensive study site. More recent campaigns, funded by the European Space Agency (ESA) for the proposed CoreH20 satellite mission, have furthered this effort in Finland and Canada. During CLPX-II, in 2007 and 2008, a sled-mounted radar system, with antennas located two meters above the snow surface, was used to collect far-field backscatter measurements throughout study sites in Colorado and Alaska.

One of the main challenges with such a measurement is stability of the radar system. Frequent calibration measurements must be made, along with ground-truth observations. The measurement must be performed in the far-field, requiring a tower platform, and these systems usually require a large amount of power (Hardy *et al.*, 2008). This complicates deployment, as most well-instrumented snow sites generally run on solar power and are remote.

14.5.2 Passive microwave

In situ passive microwave observations date back to the 1970s and, since then, there have been many field campaigns performed by different groups. Microwave radiometers on the ground have usually been collecting information at the frequencies of the sensors flying into space, namely $\approx 6-$, $\approx 10-$, $\approx 19-$, $\approx 37-$ and $\approx 85\,\text{GHz}$. Such measurements have provided crucial information for the development and testing of electromagnetic models (and theories which, in turn, support the development and refinement of retrieval schemes. Microwave radiometers are generally mounted on a tripod or a tower, and are pointed toward the target with the same incidence angle as that at which satellite data is collected ($\approx 50°$).

Measurements can also be performed in a scanning mode by changing the incidence angle from $0°$ to $90°$. Usually, the scanning incidence angles are kept between $15-20°$ and $60-70°$ for practical reasons. For low incidence angles,

the feet of the tripod might be falling within the field of view of the instrument whereas, for high incidence angles, other features along the horizon (such as mountains or trees) might also fall within the field of view. In general, when selecting the site where passive microwave observations are performed, a relatively flat topography and a homogeneous snowpack is preferable. Also, in order to minimize the effects of specular reflection (e.g., contamination of emission coming from features in front of the radiometer which reflects on the snow surface and are recorded by the instrument), it is also preferable to select the measurement area at a certain distance from surrounding mountains and/or forest. Obviously, this is not always possible, and these effects should be accounted for in the post-processing phase of the data. Measurements of the sky brightness temperature should be taken regularly for the same purposes.

Wiesmann *et al.* (1996) contains data collected from a multi-frequency (11, 21, 35, 48 and 94 GHz) system based on portable radiometers operated on several sites in the Swiss Alps. The temporal and spatial behavior of the emissivity and brightness temperature is investigated for different snow and snow-free conditions, and the passive microwave measurements are complemented by ground observations and radar measurements. The data collected within the framework of CLPX also represents a unique data set. It was collected at the LSOS site at 18.7, 23.8, 36.5, and 89 GHz (both vertical and horizontal polarizations), using the Ground Based Microwave Radiometer (GBMR-7, http://nsidc.org/data/nsidc-0165.html). Three different measurement techniques were used:

1 scans of undisturbed total snow cover;
2 angular scans with varying incidence angles (between 30° and 70°); and
3 scans of bare soil and new snow.

Snow properties (density, snow temperature, stratigraphy, snow crystal size, soil moisture) and meteorological forcing data (wind speed, wind direction, air temperature, relative humidity, downward long-wave radiation, downward short-wave radiation and precipitation) were also collected. This data was used to study melting and refreezing cycles and evaluate electromagnetic models (e.g., Tedesco *et al.*, 2006).

During CLPX, multiband polarimetric brightness temperature images over the three Meso-cell Study Areas (MSAs) were also collected (http://nsidc.org/data/nsidc-0155.html). One of the goals was to collect data at a spatial resolution representative of the topography and vegetation cover, and to provide a simulated AMSR-E microwave data set. This data set was also used to perform scaling analysis and, for example, to study the impact of vegetation on brightness temperature (Tedesco *et al.*, 2005).

Passive microwave radiometers have also been used to study to collect information over the Greenland and Antarctica ice sheets. Over Antarctica, in particular, this is performed to provide a calibration data set for a relatively *stable* target on Earth (e.g., Dome C, Antarctica). Over Greenland, microwave radiometers have been used to collect passive microwave data in proximity to the Summit station in order to understand the spatial variability of brightness temperature within a satellite footprint over relatively stable targets.

14.6 Sampling strategies for remote sensing field campaigns: concepts and examples

When comparing ground-based measurements with remote sensing observations, one must take into account the difference in the scale triplet (Bloschl, 1999):

1 the *support*, or area over which the measurement integrates;
2 the *spacing*, or distance between measurements; and
3 the spatial *extent* of the measurements.

For example, a depth probe measurement has a support of 1 cm, a typical spacing of 50 meters, and a typical extent of several kilometers. A spaceborne passive microwave brightness temperature measurement has a support of 5–50 km, a spacing equal to the support, and global extent.

In order to account for these differences in scale triplet, efficient sampling strategies are required. This section describes strategies from several example calibration/validation field campaigns. A useful reference for better understanding problems and solutions associated to the collection on ground for remote sensing validation is McCoy (2004). In the following, some examples related to specific problems in the cryosphere are reported, focusing on major campaigns. Figure 14.15 shows a suite of measurements made during a validation and calibration campaign in Svalbard. The mismatch in support, spacing, and extent, require many people on the ground during airborne and spaceborne overpasses. Performing enough measurements to accurately characterize the mean snow and ice properties at the necessary scale is challenging. Example campaigns and sampling strategies are described in the sections below.

14.6.1 Ice sheet campaigns

The CryoSat Validation EXperiement (CryoVEX) campaigns were initiated in advance of the launch of the ESA satellites CryoSat and CryoSat-2. These satellites have a single mission goal – to measure fluctuations in the thickness of sea and land ice. The key instrument on these satellites is a radar altimeter, the Synthetic aperture Interferometric Radar Altimeter (SIRAL). Because SIRAL was a new radar altimeter design, never before flown in space, simulated measurements were desirable from the variety of ice and snow conditions likely to be observed by SIRAL. This was achieved through the construction of an airborne simulator for SIRAL. The Airborne Synthetic Aperture Interferometric Radar Altimetry System (ASIRAS) was a low-altitude sensor using the same radar technology as SIRAL, flown from a fixed-wing aircraft (frequently a De Havilland Twin Otter or Dornier 228–200).

CryoVex campaigns were carried out in 2003, 2004, 2006, 2007, 2008, 2011, and 2012. The basic scheme of the campaigns was to place ground teams at representative sites around the Arctic, including several sea ice locations with different types of sea ice, small ice caps and glaciers, the margins of the Greenland Ice
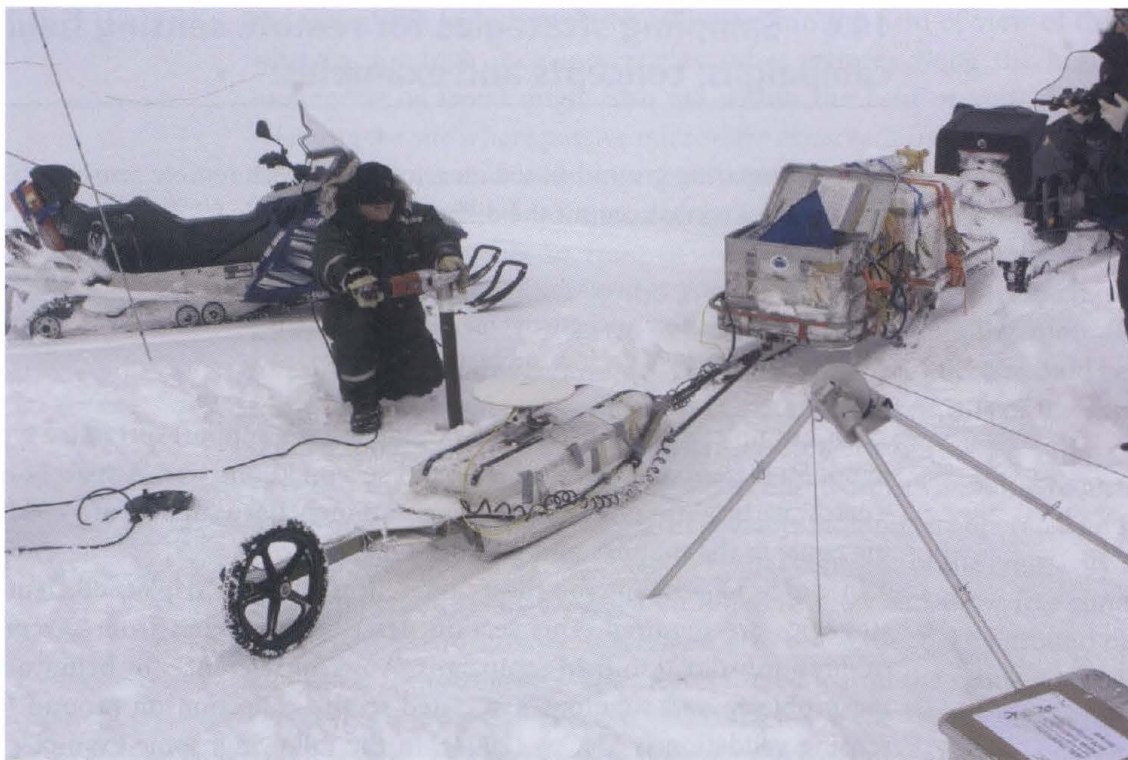
Figure 14.15 An intensive ground-truthing campaign on Kongsvegen, Svalbard. Visible in the photo are many field-measurement instruments. The sled in the center of the scene carries GPR and GPS antennas. To the left of the sled, shallow core drilling is in progress. To the right of the sled, a logging cable goes over a pulley to a Wallingford probe, measuring density in a previously drilled borehole. At the far left, a probe for measuring snow depth is ready for use.

Sheet, and its interior. At each location, tight coordination between the aircraft and ground teams allowed precise overflights of the ground measurements. Each ground team erected a corner reflector (e.g., a metallic object of specific known shape and dimensions), designed to create a powerful return, positioned above the snow surface at a measured distance. This was to determine the difference between the snow surface, as re-tracked by the radar altimeter, and the snow surface, as measured on the ground by the field teams. Absolute snow surface elevation was also measured *in situ*, using differential GPS.

In addition to the measurement of true surface height, teams carried out numerous *in situ* experiments, including detailed stratigraphy measurements in snow pits, ground-based radar measurements, detailed density profiles with shallow cores or a Neutron Probe technique (Morris and Cooper, 2003; Morris, 2008), and firn densification measurements with the "coffee can" technique (Hamilton and Whillans, 2000). On sea ice, teams measured sea ice thickness, snow depth over sea ice, absolute surface elevation, and profiles of snow and sea ice physical properties from snow pits and cores. To extend the spatial extent of sea ice thickness measurements, a helicopter with a low-altitude electromagnetic induction system flew surveys to determine sea ice thickness at larger spatial scales. The sea ice surface is extremely dynamic, changing on timescales as short

as minutes. Thus, extremely precise coordination was required to ensure that ground teams and aircraft sampled the same sea ice location at the same time.

During the CryoVEX campaigns, one key question was the *spatial variability* of the properties to be measured on the ground. Put simply, how representative is a point measurement made on the ground, in context of the larger footprint (tens of kilometers) of a spaceborne radar altimeter? To assess spatial variability on a variety of scales, a *nested grid* layout was chosen for sampling sites. In the nested grid, measurements (snow pits, cores, etc.) were collected along two perpendicular lines. At the intersection of these two lines was the first measurement. Further measurements were made along each line at distances of 1 m, 10 m, 100 m, and 1000 m. In this way, differences at several length scales, and in differing directions, could be determined.

After the launch of ICESat-1, a satellite carrying the GeoScience Laser Altimetry System (GLAS), an elevation validation campaign, was undertaken at Summit station in the center of the Greenland Ice Sheet. An orbit track (track 412) passed within 5 km of the station, and it was determined that a time series of elevation along this track would be beneficial for validation. The design of this validation measurement considered several factors. First, it was desirable for science technicians to be able to make measurements on a monthly basis, all year round. This meant the length of the measurement along-track needed to be limited to a distance that could be reasonably covered in a day, including preparation time.

Because the *support* of an ICESat-1 measurement is relatively small ($\approx$70 m spot size on the ground), and the actual pointing direction of the satellite was not precise enough to target the same track within 70 m on each orbit, a survey in a straight line along the nominal ground track would not always be coincident with satellite measurements. Furthermore, because slope is so important in interpreting elevation measurements, a characterization of the slope is desirable. The sampling strategy chosen used kinematic GPS to measure surface topography. The GPS collected data on 1 second intervals, and the antenna was mounted on a sled pulled by a snow machine, along a 10 km track that crossed the nominal ground track in a square-wave pattern. In this way, crossovers between ground-based GPS and satellite laser measurements were assured for each survey. This eliminated the need to interpolate positions because, for every campaign sampled, multiple laser "shots" were transected by intersecting GPS data (Siegfried *et al.*, 2011).

14.6.2 Seasonal snow campaigns

The Cold Lands Processes eXperiment (CLPX; http://www.nohrsc.nws.gov/~cline /clpx.html) was the first large coordinated snow remote sensing calibration/validation effort. It was designed to address questions about processes understanding, spatial and temporal variability, and uncertainty in snow estimates in the terrestrial cryosphere. This large field campaign involved researchers from many different universities and government labs, and took place in the Colorado Rockies in 2002 and 2003. In particular, CLPX aimed to develop a

strong synergism between process-oriented understanding, land surface models, and microwave remote sensing (Cline, 2000).

The primary goals of this sampling were to get accurate sample mean and variance estimates at the 1 km^2 scale in six different intensive study areas (ISAs), with a secondary goal of characterizing the spatial structure within these sites at a 100 m resolution.

Four Intensive Observing Periods (IOPs) were chosen in 2002 and 2003 (February and March) to provide information about both wet and dry snowpacks in north-central Colorado. Six different aircrafts operated during this field campaign, with both passive and active microwave sensors, gamma radiation sensors, and LiDAR. In addition, data acquisition from 12 different satellite sensors was acquired during these intensive field campaigns, using optical and passive and active microwave sensors. Ground-based observations included intensive snow sampling, soil and vegetation observations, ground-based passive and active microwave sensors, and Frequency Modulated Continuous Wave (FMCW radar. Large field teams performed coincident observations during the airborne and satellite overpasses. This dataset is archived at the National Snow and Ice Data Center, and it represents the largest single field-based snow measurement campaign to date (http://nsidc.org/data/clpx/). Figure 14.16 shows some example results from CLPX, in which ground-based radar, SMP, and standard snow pit observations are compared.

Building on the lessons learned during CLPX, a second series of smaller field campaigns took place in 2007 in Colorado and 2008 in Alaska (CLPX-II), which focused on one primary airborne radar system (NASA POLSCAT), one satellite-based sensor (TerraSAR-X), and attempted to extend the range of snowpack conditions measured during CLPX. A smaller third campaign (CLPX-III) took place in Grand Mesa, Colorado, to add a high-elevation, deeper snowpack to the database. For snow depth, wetness and surface roughness measurements, each site was stratified using a 100 m interval grid, with two orthogonal transects in each cell. The transect starting point and resolution (5, 10, 15, 20, or 25 meters) were chosen at random, with the orthogonal transects starting at the same location and with a direction based on the starting point to ensure that the transect remained within the cell. Two of the grid cells were chosen at random, and additional 25 measurements were made on a 20 m sub-grid, with the location of the measurement within each 20 m grid cell chosen at random. For snow pit observations, which are much more time-consuming, the 1 km^2 area was divided into 250 m grid cells, and a snow pit location within each cell was chosen at random.

14.6.3 Sea ice campaigns

Two major field campaigns for testing sea ice retrieval algorithms from the Advanced Microwave Scanning Radiometer (AMSR-E) were undertaken in 2003 and 2006 (AMSR-Ice03, AMSR-Ice06, http://nsidc.org/data/amsr_validation /cryosphere/amsrice03/index.html). These campaigns took place near Barrow, Alaska, on the Chukchi and Beaufort Seas and in Elson Lagoon. Extensive
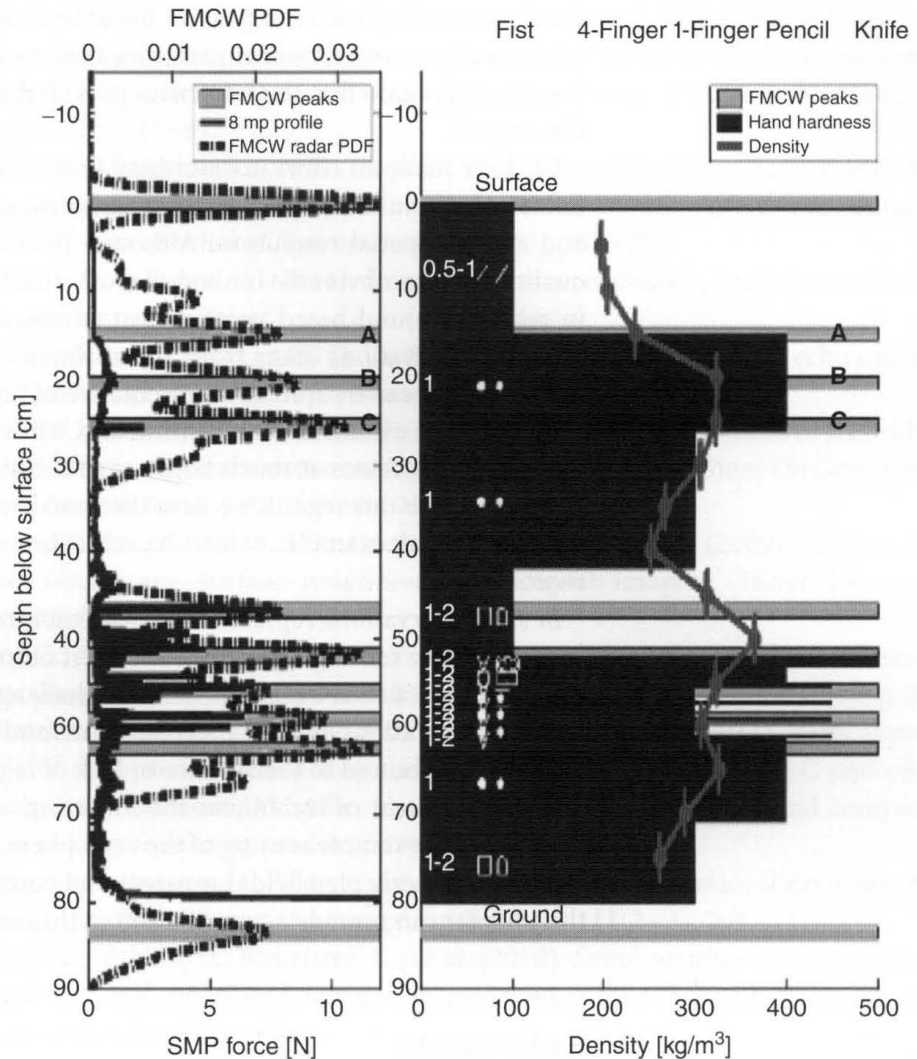
Figure 14.16 Left panel shows radar results as dashed line, SMP results as solid line, and location of major radar reflections highlighted in gray. Right panel shows snow hardness in black, density in gray, and grain size and type. Note that the major radar reflections correlate well with changes detected with other measurement techniques. (Marshall *et al.*, 2007. Reproduced with permission of Elsevier).

field-based measurements of sea ice conductivity, ocean salinity, snow depth, sea ice thickness, temperatures of the air, ice, and snow/ice interface, and surface roughness were performed. Snow pits, with stratigraphy and density, were also recorded. In 2006, the experiment was repeated in the same location, this time with an airborne microwave radar from the Center for Remote Sensing of Ice Sheets (CReSIS) for measuring snow. A similar suite of ground-based measurements was made as in 2003, with the addition of a ground-based FMCW radar mounted to a sled.

14.7 Conclusions

In this chapter, we have provided an overview of some of the physical properties of the cryosphere that are of interest for remote sensing observations. Because of the extensive number of quantities that should be discussed, and the limited

space at our disposal in a general book such as this one, we acknowledge that we might have missed some quantities that could be of interest to some readers. We sincerely hope that the references provided in the chapter will help readers in this regard.

We have made an effort in describing both established standard techniques and new state-of-the-art modern techniques for measuring physical properties rapidly and at high spatial resolution. Although *in situ* observations can provide high quality but are obviously limited in both space and time, major complications in relating ground-based point measurements of physical properties to remote sensing observations stem from the mismatch in scale. An individual *in situ* measurement can be seen as representative of physical properties at a scale of the order of a few meters or even centimeters, while remote sensing observations are affected by processes at much larger spatial scales (e.g., tens of meters to tens of kilometers). In this regard, we have discussed sampling strategies and concluded the chapter with examples of field-based calibration and validation efforts made in recent years.

In situ observations represent a crucial tool for improving, validating and calibrating remote sensing algorithms and their outputs. In the case of the cryosphere, the collection of such data is particularly challenging, in view of the difficult access to test sites locations, to the harsh conditions and cold temperatures characterizing many field sites, and to the absence or lack of logistical support. The development and advancement of techniques for collecting *in situ* data is a key factor for the progress of the remote sensing of the cryosphere, together with the training of scientists to properly plan field campaigns and perform fieldwork activities. We hope this chapter can provide a contribution in this direction.

References

Abdalati, W. & Krabill, W. (1999). Calculation of ice velocities in the Jakobshavn Isbrae area using airborne laser altimetry. *Remote Sensing of Environment*, **67**(2), 194–204.

Albert, M. & Hawley, R. (2002). Seasonal changes in snow surface roughness characteristics at Summit, Greenland: implications for snow and firn ventilation. *Annals of Glaciology* **35**(35), 510–514.

Bloschl, G. (1999). Scaling issues in snow hydrology. *Hydrological Processes*, **13**(14–15), 2149–2175.

Breton, D.J., Hamilton, G.S. & Hess, C.T. (2009). Design, optimization and calibration of an automated density gauge for firn and ice cores. *Journal of Glaciology* **55**(194), 1092–1100.

Cline, D. (2000). The NASA Cold Land Processes Mission. *Eos, Transactions, American Geophysical Union* **81**(48).

Conway, H., Catania, G., Raymond, C., Gades, A., Scambos, T. & Engelhardt, H. (2002). Switch of flow direction in an antarctic ice stream. *Nature* **419**(6906), 465–467.

Conway, H., Smith, B., Vaswani, P., Matsuoka, K., Rignot, E. & Claus, P. (2009). A low-frequency ice-penetrating radar system adapted for use from an airplane: test results from Bering and Malaspina glaciers, Alaska, USA. *Annals of Glaciology* **50**(51), 93–97.

Cuffey, K. & Paterson, S. (2010). *The physics of glaciers*, 4th edition. Academic Press.

Deems, J., Fassnacht, S. & Elder, K. (2006). Fractal distribution of snow depth from LiDAR data. *Journal of Hydrometeorology* **7**(2), 285–297.

DeWalle, D. & Rango, A. (2011). *Principles of snow hydrology*, 2nd Edition. Cambridge University Press.

Evans, S. & Robin, G.D.Q. (1972). Ice thickness measurement by radio echo sounding, 1971–1972. *Antarctic Journal of the United States* **7**(4), 108.

Farrell, S.L., Kurtz, N., Connor, L.N., *et al.* (2012). A first assessment of IceBridge snow and ice thickness data over Arctic sea ice. *IEEE Transactions On Geoscience and Remote Sensing* **50**(6), 2098–2111.

Fassnacht, S.R., Stednick, J.D., Deems, J.S. & Corrao, M.V. (2009). Metrics for assessing snow surface roughness from digital imagery. *Water Resources Research* **45**, W00D31.

Fierz, C., Armstrong, R.L., Durand, Y., *et al.* (2009). The international classification for seasonal snow on the ground. *IHP-VII Technical Documents in Hydrology* **83**.

Gallet, J.-C., Domine, F., Arnaud, L., Picard, G. & Savarino, J. (2011). Vertical profile of the specific surface area and density of the snow at Dome C and on a transect to Dumont D'Urville, Antarctica – albedo calculations and comparison to remote sensing products. *Cryosphere* **5**(3), 631–649.

Gogineni, S., Braaten, D., Allen, C., *et al.* (2007). Polar radar for ice sheet measurements (PRISM). *Remote Sensing of Environment* **111**(2–3), 204–211.

Greene, E., Atkins, D., Birkeland, K., *et al.* (2010). *Snow, weather and avalanches: observational guidelines for avalanche programs in the U.S*, 2nd Edition. American Avalanche Association.

Hamilton, G. & Whillans, I. (2000). Point measurements of mass balance of the Greenland Ice Sheet using precision vertical global positioning system (GPS) surveys. *Journal of Geophysical Research – Solid Earth* **105**(B7), 16295–16301.

Hardy, J., Davis, R., Koh, Y., *et al.* (2008). NASA Cold Land Processes Experiment (CLPX 2002/03): Local Scale Observation Site. *Journal of Hydrometeorology* **9**(6), 1434–1442.

Hawley, R., Waddington, E., Alley, R. & Taylor, K. (2003). Annual layers in polar firn detected by borehole optical stratigraphy. *Geophysical Research Letters* **30**(15), 1788.

Hawley, R.L., Brandt, O., Morris, E.M., Kohler, J., Shepherd, A.P. & Wingham, D.J. (2008). Techniques for measuring high-resolution firn density profiles: case study from Kongsvegen, Svalbard. *Journal of Glaciology* **54**(186), 463–468.

Hawley, R.L. & Waddington, E.D. (2011). *In situ* measurements of firn compaction profiles using borehole optical stratigraphy. *Journal of Glaciology* **57**(202), 289–294.

Havens, S., Marshall, H.-P., Pielmeier, C. & Elder, K. (2013). Automatic grain type classification of snow micro penetrometer signals with random forests. *Transactions on Geoscience and Remote Sensing* **51**(6), 3328–3335.

Holt, J., Blankenship, D., Morse, D., *et al.* (2006). New boundary conditions for the West Antarctic Ice Sheet: subglacial topography of the Thwaites and Smith glacier catchments. *Geophysical Research Letters.* **33**(9), L09502.

Howat, I.M., Joughin, I. & Scambos, T.A. (2007). Rapid changes in ice discharge from Greenland outlet glaciers. *Science* **315**(5818), 1559–1561.

Johnson, J.B. & Schneebeli, M. (1999). Characterizing the microstructural and micromechanical properties of snow, *Cold Regions Science and Technology*, **30**, 91–100.

Kavanagh, B.F. & Glenn Bird, S.J. (1996). *Surveying principles and applications*, 4th edition. Prentice Hall, pp. 257–264. ISBN 0-13-438300-1.

Kaempfer, T., Schneebeli, M. & Sokratov, S. (2005). A microstructural approach to model heat transfer in snow. *Geophysical Research Letters* **32**(21), L21503.

King, M. (2004). Rigorous GPS data-processing strategies for glaciological applications. *Journal of Glaciology* **50**(171), 601–607.

Lacroix, P., Legresy, B., Langley, K., *et al.* (2008). *In situ* measurements of snow surface roughness using a laser profiler. *Journal of Glaciology* **54**(187), 753–762.

Larsen, C.F., Motyka, R.J., Arendt, A.A., Echelmeyer, K.A. & Geissler, P.E. (2007). Glacier changes in Southeast Alaska and Northwest British Columbia and contribution to sea level rise. *Journal of Geophysical Research – Earth Surface* **112**(F1), F01007.

Loewe, H. & van Herwijnen, A. (2012). A poisson shot noise model for micro-penetration of snow. *Cold Regions Science and Technology* **70**, 62–70.

Lomonaco, R., Albert, M. & Baker, I. (2011). Microstructural evolution of fine-grained layers through the firn column at Summit, Greenland. *Journal of Glaciology* **57**(204), 755–762.

Lutz, E., Birkeland, K. & Marshall, H.-P. (2009). Quantifying changes in weak layer microstructure associated with artificial load changes. *Cold Regions Science and Technology* **59**(2–3), 202–209.

Mankoff, K.D., Russo, T.A., Norris, B.K., *et al.* (2011). Kinects as sensors in earth science: glaciological, geomorphological, and hydrological applications. *Eos, Transactions, American Geophysical Union* (Abstract #C41D-0442).

Marshall, H.P., Schneebeli, M. & Koh, G. (2007). Snow stratigraphy measurements with high-frequency FMCW radar: comparison with snow micropenetrometer. *Cold Regions Science and Technology* **47**, 108–117.

Marshall, H.-P. & Koh, G. (2008). FMCW radars for snow research. *Cold Regions Science and Technology* **52**(2), 118–131.

Marshall, H.-P. & Johnson, J.B. (2009). Accurate inversion of high-resolution snow penetrometer signals for microstructural and micromechanical properties. *Journal of Geophysical Research – Earth Surface* **114**, F04016.

Matzl, M. & Schneebeli, M. (2006). Measuring specific surface area of snow by near-infrared photography. *Journal of Glaciology* **52**(179), 558–564.

Matzler, C., Strozzi, T., Weise, T., Floricioiu, D. & Rott, H. (1997). Microwave snowpack studies made in the Austrian Alps during the SIR-C/X-SAR experiment. *International Journal of Remote Sensing* **18**(12), 2505–2530.

McClung, D.M. & Schaerer, P.A. (1993). *The Avalanche Handbook*. The Mountaineers, Seattle, WA.

McCoy, R. (2004). *Field Methods in Remote Sensing*. The Guilford Press, ISBN10 1593850794.

Morris, E.M. (2008). A theoretical analysis of the neutron scattering method of measuring snow and ice density. *Journal of Geophysical Research – Earth Surface* **113**(F4), F04099.

Morris, E. & Cooper, J. (2003). Instruments and methods – density measurements in ice boreholes using neutron scattering. *Journal of Glaciology* **49**(167), 599–604.

Nereson, N. & Raymond, C. (2001). The elevation history of ice streams and the spatial accumulation pattern along the Siple Coast of West Antarctica inferred from ground-based radar data from three inter-ice-stream ridges. *Journal of Glaciology* **47**(157), 303–313.

Painter, T.H., Molotch, N.P., Cassidy, M., Flanner, M. & Steffen, K. (2007). Instruments and methods – contact spectroscopy for determination of stratigraphy of snow optical grain size. *Journal of Glaciology* **53**(180), 121–127.

Paul, F. & Haeberli, W. (2008). Spatial variability of glacier elevation changes in the Swiss Alps obtained from two digital elevation models. *Geophysical Research Letters* **35**(21), L21502.

Pielmeier, C., Schneebeli, M. & Stucki, T. (2001). Snow texture: a comparison of empirical versus simulated texture index for alpine snow. *Annals of Glaciology* **32**, 7–13.

Pielmeier, C. & Marshall, H.-P. (2009). Rutschblock-scale snowpack stability derived from multiple quality-controlled snowmicropen measurements. *Cold Regions Science and Technology* **59**(2–3), 178–184.

Robin, G.D.Q., Evans, S. & Bailey, J.T. (1969). Interpretation of radio echo sounding in polar ice sheets. *Philosophical Transactions of the Royal Society of London Series A – Mathematical and Physical Sciences* **265**(1166), 437–505.

Satyawali, P.K. & Schneebeli, M. (2010). Spatial scales of snow texture as indicator for snow class. *Annals of Glaciology* **51**, 55–63.

Satyawali, P.K., Schneebeli, M., Pielmeier, C., Stucki, T. & Singh, A.K. (2009). Preliminary characterization of alpine snow using snowmicropen. *Cold Regions Science and Technology* **55**, 311–320.

Schneebeli, M., Coleou, C., Touvier, F. & Lesaffre, B. (1998). Measurement of density and wetness in snow using time-domain reflectometry. *Annals of Glaciology* **26**, 69–72.

Schneebeli, M. & Sokratov, S. (2004). Tomography of temperature gradient metamorphism of snow and associated changes in heat conductivity. *Hydrological Processes* **18**(18), 3655–3665.

Siegfried, M.R., Hawley, R.L. & Burkhart, J.F. (2011). High-resolution ground-based GPS measurements show intercampaign bias in ICESat elevation data near Summit, Greenland. *IEEE Transactions On Geoscience and Remote Sensing* **49**(9), 3393–3400.

Strozzi, T. & Matzler, C. (1998). Backscattering measurements of alpine snowcovers at 5.3 and 35 GHz. *IEEE Transactions On Geoscience and Remote Sensing* **36**(3), 838–848.

Tedesco, M., Kim, E., Gasiewski, A., Klein, M. & Stankov, B. (2005). Analysis of multiscale radiometric data collected during the Cold Land Processes Experiment-1 (CLPX-1). *Geophysical Research Letters* **32**(18), L18501.

Tedesco, M., Kim, E.J., England, A.W., De Roo, R.D. & Hardy, J.P. (2006a). Brightness temperatures of snow melting/refreezing cycles: observations and modeling using a multilayer dense medium theory-based model. *IEEE Transactions On Geoscience and Remote Sensing* **44**(12), 3563–3573.

Tedesco, M., Kim, E., Cline, D., *et al.* (2006b). Comparison of local scale measured and modelled brightness temperatures and snow parameters from the CLPX 2003 by means of a dense medium radiative transfer theory model. *Hydrological Processes* **20**(4), 657–672.

Trujillo, E., Ramirez, J.A. & Elder, K.J. (2007). Topographic, meteorologic, and canopy controls on the scaling characteristics of the spatial distribution of snow depth fields. *Water Resources Research* **43**(7), W07409.

Trujillo, E., Ramirez, J.A. & Elder, K.J. (2009). Scaling properties and spatial organization of snow depth fields in sub-alpine forest and alpine tundra. *Hydrological Processes* **23**(11), 1575–1590.

Ulaby, F.T., Stiles, W.H., Dellwig, L.F. & Hanson, B.C. (1977). Experiments on radar backscatter of snow. *IEEE Transactions On Geoscience and Remote Sensing* **15**(4), 185–189.

Vaughan, D.G., Corr, H.F.J., Smith, A.M., Pritchard, H.D. & Shepherd, A. (2008). Flow-switching and water piracy between Rutford Ice Stream and Carlson Inlet, West Antartica. *Journal of Glaciology* **54**(184), 41–48.

Waddington, E.D., Neumann, T.A., Koutnik, M.R., Marshall, H.-P. & Morse, D.L. (2007). Inference of accumulation-rate patterns from deep layers in glaciers and ice sheets. *Journal of Glaciology* **53**(183), 694–712.

Waite, A.H. & Schmidt, S.J. (1962). Gross errors in height indication from pulsed radar altimeters operating over thick ice or snow. *Proceedings of the Institute of Radio Engineers* **50**(6), 1515.

Wiesmann, A., Strozzi, T. & Weise, T. (1996). *Passive microwave signature catalogue of snowcovers at 11, 21, 35, 48 and 94 GHz*. Institute of Applied Physics (IAP), University of Bern, IAP-Report 96-8.

Acronyms

AMSR-E	Advanced Microwave Scanning Radiometer
ASIRAS	Airborne Synthetic Aperture Interferometric Radar Altimetry System
AWSs	Automated Weather Stations
BOS	Borehole Optical Stratigraphy

CLPX	NASA Cold Lands Processes Experiment
CryoVEX	CryoSat Validation EXperiement
DEMs	Digital elevation models
EDM	Electronic Distance Measurement
ESA	European Space Agency
FCC	Federal Communications Commission
GNSSs	Global Navigation Satellite Systems
GPS	Global Positioning System
IOPs	Four Intensive Observing Periods
ISAs	Intensive study areas
LiDAR	Light Detection And Ranging
LSOS	Local Scale Observation Site
MABLE	Mostly Automated Borehole Logging Experiment
MADGE	Maine Automated Density Gauge Experiment
MSAs	Meso-cell Study Areas
NAVSAT	Navy Navigation Satellite System
NIR	Near InfraRed
PPK	Post-processed kinematic
RTK	Real-time kinematic
SIRAL	Synthetic aperture Interferometric Radar Altimeter
SMP	Snow micro-penetrometer
SSA	Specific Surface Area
SWE	Snow water equivalent

Websites cited

http://climate2.jpl.nasa.gov/ice/missions/
http://www.nasa.gov/mission_pages/icebridge/index.html
http://en.wikipedia.org/wiki/Global_Positioning_System
http://www.wcc.nrcs.usda.gov/snow/
http://www.nasa.gov/mission_pages/icebridge/index.html
http://nsidc.org/data/nsidc-0155.html
http://www.nohrsc.nws.gov/~cline/clpx.html
http://nsidc.org/data/clpx/
http://nsidc.org/data/amsr_validation/cryosphere/amsrice03/index.html
http://nsidc.org/data/amsr_validation/cryosphere/amsrice03/index.html
http://nsidc.org/data/amsr_validation/cryosphere/amsrice03/index.html